Int J Pharm Bio Sci 2012 July; 3(3): B 346 - 354

Research Article **Molecular Biology**

International Journal of Pharma and Bio Sciences **ISSN 0975-6299**

FUNCTIONAL INTERPRETATION OF STRUCTURE OF *BACILLUS THURINGIENSIS DENDROLIMUS* T84A1-Cry1Aa9 TOXIN USING COMPUTATIONAL MODELING APPROACH

S. KASHYAP*

National Bureau of Agriculturally Important Microorganisms (ICAR), Kusmaur, Kaithauli, Mau Nath Bhanjan-275101, India.

ABSTRACT

The theoretical homology based structural model of Cry1Aa9 δ-endotoxin produced by *Bacillus thuringiensis dendrolimus* T84A1was predicted using the Cry1Aa template (Resolution 2.25Å). The Cry1Aa9 resembles the template structure by sharing a common three domains extending conformation structure responsible in pore-forming and specificity determination. The novel structural differences found are presence of β0 and β12b, absence of α7b, β1a, α9a, β9 and α11a. These increments of 3D structure information will be helpful in the design of domain swapping experiments aimed at improving toxicity, and will help in elucidation of the common mechanism of toxins action.

KEYWORDS: **Three-dimensional structure, Homology modeling, Cry1Aa9, *Bacillus thuringiensis dendrolimus* T84A, third party annotation.**

Dr.S. KASHYAP
National Bureau of Agriculturally Important Microorganisms (ICAR), Kusmaur, Kaithauli, Mau Nath Bhanjan-275101, India

INTRODUCTION

An insecticidal crystal protein produced by the soil bacterium *Bacillus thuringiensis* (Bt) belongs to a large toxin family with a target spectrum spanning insects, nematodes, flatworm and protozoa[1]. In nature Cry toxins are produced as crystalline protoxin (hence named Cry protein) within Bt sporangia and after ingestion by a susceptible insect larva, these protoxins are solubilized and proteolytically cleaved into a active toxin fragment that binds to high affinity receptors and later get inserted in the brush border epithelium. The insertion of toxin creates pores in the cell membrane causes leaching of the cellular electrolytes. This disruption causes cell lyses and finally larval death[2]. So far Cry1 toxins have extensively been used in studies of insect control either as transgenic spores or as spray formulations. Crystal structures of the active toxins in solutions have been analyzed for Cry1Aa[3] by X-ray diffraction crystallography, but structural information for other group members is severely lacking. Therefore, as an increment in structure elucidation, we report model of the Cry1Aa9 toxin based on the hypothesis of structural similarity with Cry1Aa toxin. This model supports existing hypotheses of receptor insertion and will further provide an initiation point for the Domain mutagenesis experiments among different Cry toxins.

MATERIALS AND METHODS

The amino acid sequence of the putative Cry1Aa9 protein of *Bacillus thuringiensis dendrolimus* T84A1 was retrieved from using the NCBI database sequence BAA77213[4, 5]. It was ascertained that the three dimensional structure of the protein was not available in the protein data bank, hence the present exercise of developing the three dimensional model was undertaken. The protein was composed of 570 amino acid of length. A further attempt was made for a suitable template searching using mGenTHREADER (http://cms.cs.ucl.sc.uk:3000/psipred), which is an online tool for searching similar sequences, based on sequence and structure wise similarity. From the homologous searching Cry1Aa (PDB: 1CIY, resolution 2.25Å) was selected as template protein.

The three dimensional structure of target protein was predicted by using the alignment between the target (Cry1Aa9) and template protein and running it in MODRLLER software[6]. The resulted theoretical model was subjected to a series of tests for evaluating its consistency and reliability. Backbone confirmation was evaluated by the inspection of the Psi/Phi Ramachandran plot from RAMPAGE web server (http://mordred.bioc.cam.ac.uk/).

The energy criterion was evaluated by ProSA web server (https://prosa.services.came.sbg.ac.at) which compares the potential of mean forces derived from a large set of NMR and X-ray Crystallographically derived protein structures of similar sizes. Potential deviations were calculated with SUPERPOSE web server (http://wishart.biology.ualberta.ca/cgi-bin/) for root mean square deviaions (RMSD) between target and template protein structures. The visualization and refinement of model performed on UCF Chimera software (http://www.cgl.ucsf.edu/chimera) and PyMOL 0.99rc6 (http://www.pymol.org/funding.html) loaded on a personal computer machine having an Intel Quad core processer and four gigabytes of random accessed memory. Figures and electrostatic potentials calculations were generated with PyMOL0.99rc6.

RESULTS AND DISCUSSION

Based on structural alignment of the amino acid sequence between the Cry1Aa9 with Cry1Aa a theoretical model for the Cry1Aa9 toxin was obtained corresponds to residues 82-652 of the primary structure (Fig.1).

Three dimensional, three domain structure of the Cry1Aa9 toxin oligomer.

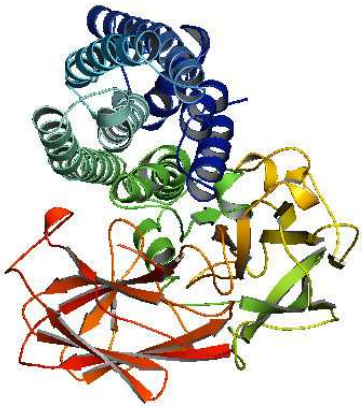

Figure 1
Three dimensional, three domain structure of the Cry1Aa9 toxin oligomer. Complete molecular view from top showing helical pore forming domain and the lower antiparellel nature of sheets arrangement.

Alignment of domain I was straightforward and the highly conserved nature of helix made placement of the residues in this domain possible. Similar alignment of domain II was also reliable within the possible limits of flanking domains I and III. No substantial insertion or deletion has to be performed in the overall sequence due to high homology between the template and the target sequence and lengths of each domain were determined by selecting the combination that allowed the best conservative profile of the neighboring amino acids. Domain III is quite well conserved both on the N-terminal and C-terminal sides. The domain I is composed of residues 82-316 and consists of 9 α-helices and two small β-strands. All the helices in the Cry1Aa9 model were slightly shorter than those in Cry1Aa. According to the amphiphilicity calculated with the Hoops and Woods values, the most exposed helices are α1, α2a, α2b, α3 and α6, which correspond well with the accessibility calculated with SwissPDB, except for α1, which is packed against domain II (Fig. 2).

Surface structure of the Cry1Aa9 oligomer

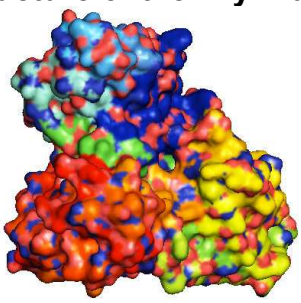

Figure 2
The three dimensional, three domain surface structure of the Cry1Aa9 oligomer.

It is possible that this helix will have some mobility, if we take into consideration that one of the cutting sites by gut proteases is located close to the middle of this helix[7]. On the other hand, membrane insertion and pore formation are thought to occur through elements of the

domain I, composed of a bundle of six amphipathic α-helices surrounding the highly hydrophobic helix α5[8, 9]. Spectroscopic studies with synthetic peptides corresponding to the domain I helices revealed that α4 and α5 have the greatest propensity for insertion into artificial membranes, although insertion and pore formation were more efficient when α4 and α5 were connected by a segment analogous to the α4-α5 loop of the toxin[10, 11]. A particularly large number of single-site mutations with altered amino acids from these helices, which lead to a strong reduction in the toxicity and pore-forming ability of the toxin, have been characterized[12, 13, 14, 15]. Also, a site-directed chemical modification study has provided strong evidence that α4 lines the lumens of the pores formed by the toxin[16]. Recent studies have established that toxin activity is especially sensitive to modifications not only in the charged residues of α4[15] but in most of its hydrophilic residues[12]. Furthermore, the loss of activity of most of these mutants did not result from an altered selectivity or size of the pores but from a reduced pore-forming capacity of the toxin[20]. The charge distribution pattern in the Cry1Aa9 theoretical model corresponds to a negatively charged patch along β4 and β13 (Fig.3) of domains II and III respectively.

The distribution of charge along Cry1Aa9 surface

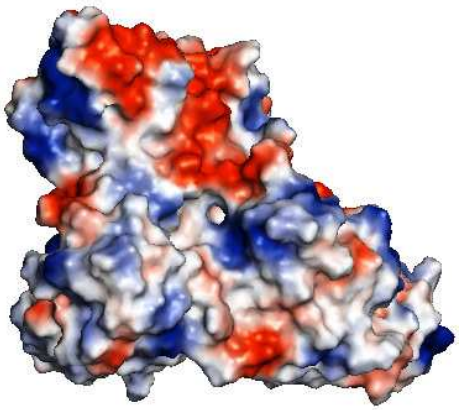

Figure 3
The localized charge distribution pattern along Cry1Aa9 oligomer showing negative patch (blue) at their end. The color scale is Red (+10) and Blue (-10).

The Cry1Aa9 domain I model relates well with data from Gazzit et al.[11] who suggested that α4 and α5 insert into the membrane in an antiparallel manner as a helical hairpin. It is possible that according to the surface electrostatic potential of helices 4 and 5, there was a neutral region in the middle of the helices which probably indicates, if the umbrella model is correct, that both helices cross the membrane with their polar sides exposed to the solvent, as it has been suggested by the results of mutagenesis experiments performed by Kumar and Aronson[13] with the Cry1Ac toxin. This region is also the most conserved among the Cry toxins. Kumar and Aronson[13] demonstrated that mutations in the base of helix 3 and the loop between α3 and α4 that cause alterations in the balance of negative charged residues may cause loss of toxicity. Mutations in helices α2, α6 and α3 (surface residues) did not substantially gtrnaslates into toxicity, while helices α4 and α5 are very sensitive to mutational alterations. Helix α1 probably does not play an important part in toxin activity after cleavage of the protoxin. It is possible that mutations aimed to an increase in amphilicity in

these helices will improve the pore forming activity of Cry1Aa9 type of toxins. As for other Cry toxins, domain II of the Cry1Aa9 toxin consists of three Greek key beta sheets arranged in a beta prism topology. It is comprised of residues 318-521, one helix (α8) and 11 β-strands. In the case of the three domain Cry toxins, specificity is mostly attributed to their capacity to bind to certain proteins located on the surface of the intestinal membrane through specific segments of domains II and III, composed mainly of β sheets[17, 18].

Loop β4-β5 is mostly hydrophilic, and the charged residues located at the tip of the loop are probably important determinants of insect specificity. As in loop β2-β3, a glycine residue is also present before a negatively charged residue supporting the hypothesis that correct orientation of charged residues in the specificity loops could be important in receptor recognition. Mutations in defined regions of the Cry1Aa toxin have identified residues 365-371 (equivalent to residues 436-442 in the Cry1Aa9 β6-β7 loop), as essential for binding to the membrane of midgut cells of *Bombyx mori*[19, 20]. In the Cry1Aa9 model, this region is shorter than their counterparts in Cry1Aa. Loop β2-β3 seems also to be able to modulate the toxicity and specificity of Cry1C [21]. The dual specificity of Cry2Aa for Lepidoptera and Diptera has been mapped to residues 307-382 that corresponds in the Cry1Aa9 theoretical model to sheet 1, strand β6, and loop β6-β7, where most of the insertions/deletions and structural differences were located. Domain III comprised by residues 533-652 and showed high conservation of residues and the only important modification is a 3-residue deletion between β16 and β17.

Several studies indicate that site mutations in this block reduce toxicity and alter channel properties in Cry1Ac[19] and Cry1Aa[22, 23], divergence in block 5 possibly reveals an alternative mechanism of membrane permeabilization.

In conclusion, evidences presented here, based on the identification of structural equivalent residues of Cry1Aa in Cry1Aa9 toxin through homology modeling indicate that, due to high amino acid homology among these two toxins, they do share a common three-dimensional structure (Fig. 2). Cry1Aa and Cry1Aa9 contain the most variable regions in the loops of domain II, which is responsible for the specificity of these toxins. Structural comparison indicates a correspondence to the general model for a Cry protein (an α+β structure with three domains) and the few of the differences present are presented of β0 and β12b, absence of α7b, β1a, α9a, β9, α11a (Table 1). Finally, the superimposed backbone traces showed low RMS deviations (Fig. 4).

The comparison between the overall energy of developed structure with those of experimentally determined structures in PROSA database validated the developed model as folded near to experimentally determined, natural structures (Fig. 5) while the Ramachandran plot analysis (Fig. 6) supported the above conclusions by showing that most of the residue (99%) has ϕ and ψ angles in the core- and in allowed-regions, except six residues which qualifies for outlier region. Most of the bond lengths, bond- and torsion-angles; are in the range of values which are expected for a naturally folded protein. This is the first model of a Cry1Aa9 protein and its importance can be perceived since members of this group of toxins are potentially important entamopathogenic candidates.

SuperPose analyses of developed structure

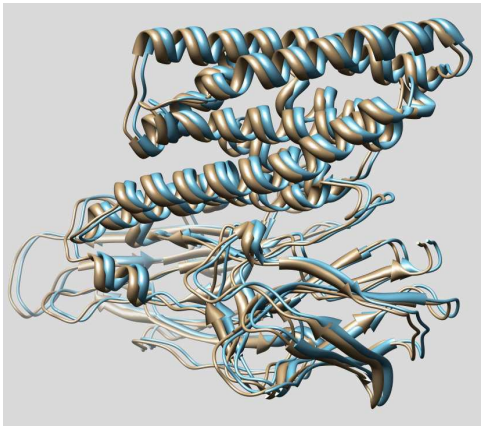

Figure 4
Superpose backbone 3d structure of Cry1Aa1 (Yellow) and Cry1Aa9 (blue) showing low structural deviations between reference and generated model.

Table 1

	*Cry*1Aa	*Cry*1Ab9		*Cry*1Aa	*Cry*1Ab9		*Cry*1Aa	*Cry*1Ab9
	Domain I			**Domain II**			**Domain III**	
α1	Pro82-Ser95	Pro82 – Ser95	**α8a**	Pro271-Glu274	Pro318-Asn322	**α11a**	Leu475-Lys477	Thr536-Leu528
α2a	Aln101-Trp112	Ala101 –Trp112	**α8b**	Ala284-Gln289	Met330-Asn337	**β13a**	Ser486-Val488	Ser533-Val535
α2b	Pro117-Ile112	Pro117- Ile 131	**β2**	Asp298-His310	Ile346-His357	**β13b**	Ile498-Arg 501	Ile545-Arg548
α3	Glu90-Ala119	Glu137-Ala166	**β3**	Phe313-Trp316	Phe360-Ser371	**β14**	Gly505-Asn513	Gly552-Asn560
α4	Pro124-Leu148	Pro171-Phe195	**β4**	Gly318-Pro325	Val395-Ser398	**β15**	Tyr522-Ser530	Tyr569-Ser577
α5	Gln154-Gla180	Gln201-Trp229	**α9a**	Val326-Phe328	--	**β16**	Leu534-Ile540	Leu581-Ile587
α6	Ala186-Val218	Ala233-Val265	**α9b**	--	--	**β17**	Arg543-Phe550	Arg590-Phe597
α7a	Ser223-Thr239	Ser270-Tyr297	**β5**	Val348-Ser351	Phe405-Arg414	**α12a**	Ser562-Ser564	Ser609-Ser611
α7b	Leu241-Tyr250	--	**β6**	Ile357-Arg367	Leu427-Phe437	**β18**	Arg566-Gly569	Arg613-Gly616
β0	--	Ile314-Thr316	**β7**	Leu380-Leu383	Thr447-Tyr449	**β19**	Ser580-His588	Ser627-His635
β1a	Glu266-Thr269	--	**β8**	Gly385-Phe390	Thr454-Asp456	**β20**	Val596-Pro605	Val643-Pro652
			β9	Thr400-Tyr402	--	**β21**	--	
			α10a	Ser410-Asp412	Ser457-Val460			
			α10b	Pro423-Gly426	Pro470-Gly473			
			β10	His429-Val434	His476-Val481			
			β11	Phe452-His456	Thr493-Arg495			
			β12a	Thr471-Pro474	Phe499-His503			
			β12b	--	Thr518-Pro521			

(--: similar component not present, *Components in Italics are spatially present at downstream sites.)

ProSA analyses of developed structure

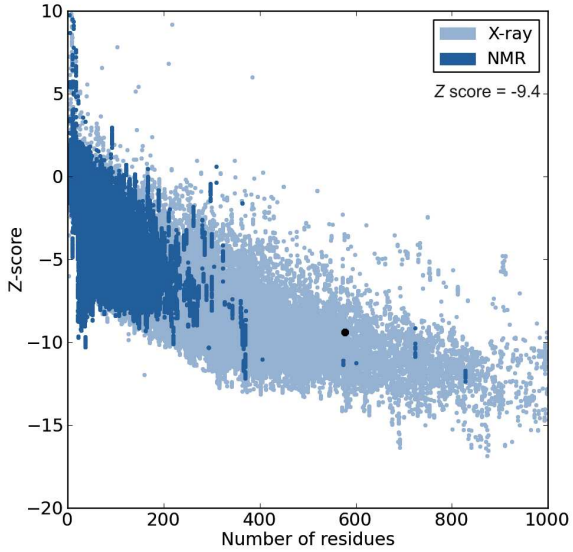

Figure 4

Model validation of Cry1Aa9 with ProSA. The result shows that the structure has features characteristic of native structures. The Z-score of -9.4 is highlighted with a large dot.

Ramachandren plot analysis of residues in deduced model

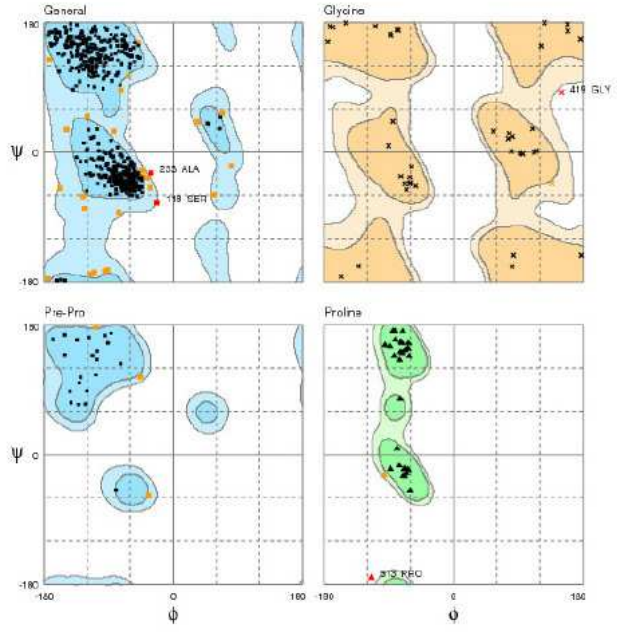

Figure 5

Ramachandren plot analysis showing placement of residues in deduced model. The structure orientation residues are separately considered for angle and torsions.

ACKNOWLEDGEMENTS

The author is grateful to ICAR for fellowship. Infrastructure facility and encouragement of the Director, NBAIM is duly acknowledged.

REFERENCES

1. Roh J. Y., Choi, J. Y., Li M. S., Jin B. R., Je Y. H., *Bacillus thuringiensis* as a specific, safe, and effective tool for insect pest control. Microbiol Biotechnol, 17: 547–559, (2007)
2. Hoffmann C., Vanderbruggen H., Hofte H., Van Rie J., Jansens, S & Van Mellaert, H., Specificity of *Bacillus thuringiensis* delta-endotoxins is correlated with the presence of high-affinity binding sites in the brush border membrane of target insect midgets. Proc Nat Acad Sci USA, 85: 7844–7848, (1988)
3. Knowles B. H., Ellar D. J. Colloid osmotic lysis is a general feature of the mechanism of action of *Bacillus thuringiensis* delta-endotoxins with different inect specificities, *Biochim* Biophys Acta, 924: 509–518, (1987)
4. Nagamatsu Y., Itai Y., Hatanaka C., Funatsu G. and Hayashi K., A Toxic Fragment from the Entomocidal Crystal Protein of Bacillus thuringiensis. Agric Biol Chem, 48: 611-619, (1984)
5. Ogo M., Yamada S., Kobayashi Y., Shibata J. and Nagamatsu,Y., Nucleotide Sequence of the Lepidoptera-toxic Protein Gene of Bacillus thuringiensis subsp. dendrolimus T84A1J. Fac. Appl. Biol. Sci., Hiroshima Univ, 29: 95-107, (1990)
6. Sali A., Potterton L., Yuan F., van Vlijmen H. and Karplus M., Evaluation of comparative protein modeling by MODELLER. Proteins, 23: 318-326, (1995)
7. Segura C., Guzman F., Patarroyo M. E., Orduz S., Activation pattern and toxicity of the Cry1Ab15Bb toxin of *Bacillus thuringiensis* subsp. Medellin. J Invertebr Pathol, 76: 56-62, (2000)
8. Grochulski P., Masson L., Borisova S., Pusztai-carey M., Schwartz J., Brousseau R. and Cygler M., *Bacillus thuringiensis* CryIA(a) insecticidal toxin: crystal structure and channel formation. J Mol Biol, 254: 447–464, (1995)
9. Li J., Carroll J., Ellar D. J. Crystal structures of insecticidal δ-endotoxin from *Bacillus thuringiensis* at 2.5 Å resolutions. Nature, 353: 815-821, (1991)
10. Gerber D. and Shai Y., Insertion and organization within membranes of the δ-endotoxin pore-forming domain, helix 4-loop-helix 5, and inhibition of its activity by a mutant helix 4 peptide. J Biol Chem, 275: 23602–23607, (2000)
11. Gazit E., La Rocca P., Sansom M. S. P., Shai Y., The structure and organization within the membrane of the helices composing the pore forming domain of *Bacillus thuringiensis* δ-endotoxin are consistent with an “umbrella-like” structure of the pore. Proc Nat Acad Sci USA, 95: 12289– 12294, (1998)
12. Girard F., Vachon V., Pre´fontaine G., Marceau L., Su Y., Larouche G., Vincent C., Schwartz J.-L., Masson L. and Laprade R., Cysteine scanning mutagenesis of α4, a putative pore-lining helix of the *Bacillus thuringiensis* insecticidal toxin Cry1Aa. Appl Environ Microbiol, 74: 2565–2572, (2008)
13. Kumar A. S. M. and Aronson A. I., Analysis of mutations in the pore-forming region essential for insecticidal activity of a *Bacillus thuringiensis* δ-endotoxin. J Bacteriol, 181: 6103–6107, (1999)
14. Nunez-Valdez M. –E., Sanchez J., Lina L., Guereca L. and Bravo. A., Structural and functional studies of a-helix 5 region from *Bacillus thuringiensis* Cry1Ab δ-endotoxin.

Biochim Biophys Acta, 1546: 122–131, (2001)

15. Vachon V, Pre´fontaine G., Rang C., Coux F., Juteau M., Schwartz J.-L., Brousseau R., Frutos R., Laprade R. and Masson. L., Helix 4 mutants of the *Bacillus thuringiensis* insecticidal toxin Cry1Aa display altered pore-forming abilities. Appl Environ Microbiol*,* 70: 6123–6130, (2004)
16. Masson L., Tabashnik B. E., Liu Y.-B., Brousseau R. and Schwartz J.-L., Helix 4 of the *Bacillus thuringiensis* Cry1Aa toxin lines the lumen of the ion channel. J Biol Chem*,* 274: 31996–32000, (1999)
17. Go´mez I., Pardo-Lo´pez L., Munoz-Garay C., Fernandez L. E., Pe´rez C., Sa´nchez J., Sobero´n M. and Bravo A., Role of receptor interaction in the mode of action of insecticidal Cry and Cyt toxins produced by *Bacillus thuringiensis*. Peptides, 28: 169–173, (2007)
18. Pigott C. R. and Ellar D. J., Role of receptors in *Bacillus thuringiensis* crystal toxin activity. Microbiol Mol Biol Rev, 71: 255–281, (2007)
19. Ge A. Z., Sivarova N. I. and Dean D. H., Location of the *Bombyx mori* specificity domain of *Bacillus thuringiensis* δ -endotoxin protein. Proc Nat Acad Sci USA, 86: 4037-4041, (1989)
20. Lu H., Rajamohan F. and Dean D. H., Identification of amino acid residues of *Bacillus thuringiensis* δ -endotoxin CryIA(a) associated with membrane binding and toxicity to Bombyx mori. J Bacteriol, 176: 5554-5559, (1994)
21. Smith G. P., Ellar D. J., Mutagenesis of two surface exposed loops of the *Bacillus thuringiensis* CryIC δ -endotoxin affects insecticidal specificity. Biochem J*,* 302: 611-616, (1994)
22. Chen X. J., Lee M. K., Dean D. H., Site-directed mutations in a highly conserved region of Bacillus *thurngiensis* δ-endotoxin affect inhibition of short circuit current across *Bombyx mori* midgets. Proc Nat Acad Sci USA, 90: 9041-9045, (1993)
23. Schwartz J. L., Potvin L., Chen X. J., Brousseau R., Laprade R., Dean D. H., Single-site mutations in the conserved alternating-arginine region affect ion channels formed by CryIAa, a *Bacillus thuringiensis* toxin. Appl Environ Microbiol*,* 63: 3978-3984, (1997)
24.